

Article

Effects of Surface Roughness and Force of Electrode on Resistance Spot Weldability of Aluminum 6061 Alloy

Hyeonggeun Jo ^{1,2}, Dongcheol Kim ¹, Munjin Kang ¹, Junhong Park ² and Young-Min Kim ^{1,*}

¹ Joining R&D Group, Korea Institute of Industrial Technology, 156 Gaetbeol-ro (Songdo-dong), Yeonsu-Gu, Incheon 21999, Korea; geun93@kitech.re.kr (H.J.); dckim@kitech.re.kr (D.K.); moonjin@kitech.re.kr (M.K.)

² Department of Mechanical Convergence Engineering, Hanyang University 222 Wangsimni-ro, Seongdong-gu, Seoul 04763, Korea; parkj@hanyang.ac.kr

* Correspondence: ymkim77@kitech.re.kr; Tel.: +82-32-850-0232

Received: 3 September 2019; Accepted: 16 September 2019; Published: 20 September 2019

Abstract: The effects of electrode surface roughness and force on the resistance spot weldability and sticking of the electrode during resistance spot welding (RSW) of aluminum 6061-T6 alloy were investigated. RSW was carried out using an as-received electrode and an abraded electrode polished with sandpaper, and the nugget size and properties such as tensile shear strength and hardness of the resulting welds were investigated at two different electrode forces. In addition, a continuous RSW process was performed on the alloy to observe the effect of the electrode surface roughness on electrode sticking. When RSW was performed using the abraded electrode, which had a rough surface, the contact resistance decreased because of the effective removal of the oxide film from the surface of the aluminum alloy; consequently, the heat generated by the resistance on the surface was reduced. In addition, the growth rate of the weld nuggets formed with the abraded electrode in the thickness direction was lower than that of the nuggets formed with the as-received electrode, and the sticking of the abraded electrode was comparatively less. Also, the influence of the electrode force on the sticking of the electrode was greater in the case of the as-received electrode.

Keywords: resistance spot welding (RSW); aluminum alloy; tensile shear strength; nugget size; sticking; surface roughness; electrode force

1. Introduction

Because of the growing concern of global warming, much efforts are being made in the automotive industry to improve fuel efficiency and reduce emissions. In addition, since various demands of consumers for safety and convenience in the automobile industry can be met by increasing the weight of the vehicle, the automobile industry is in urgent need of reducing the weight of automobile parts. Among the various weight reduction options, reducing the weight of the structure is not easy, as this would require changes in design which are difficult to introduce. In addition, since the weight reduction of the construction needs large-scale facility investments, the weight reduction of the material has attracted attention recently. If the weight of a car body is reduced by 10%, fuel efficiency can be improved by up to 6%; therefore, automakers are increasingly using ultra-high-strength steel and light materials [1]. Aluminum alloys are one of the most widely used light metals because of their excellent specific strength and comparatively low material cost. In addition, they possess excellent corrosion resistance, thermoelectric conductivity, and recyclability, and 40% weight reduction can be achieved when they are used as automotive materials.

Various methods such as arc welding, resistance spot welding (RSW), laser welding, ultrasonic welding, brazing, and mechanical bonding methods such as riveting and bolting can be applied for the joining of an aluminum alloy. Until now, research on joining of aluminum alloys has mainly focused on friction stir welding (FSW) and mechanical joining methods. Some studies were also carried out on the dissimilar joining of an aluminum alloy and steel [2]. RSW is one of the most commonly used joining processes in the automotive industry and has advantages of being cheap, fast, and easy to automate. However, performing RSW on aluminum alloys for car bodies is difficult because of the following reasons. Aluminum alloys have lower bulk resistance and higher thermal and electrical conductivities than steel; therefore, compared to steel, aluminum alloys need two- or three-time higher welding currents. In addition, aluminum readily reacts with oxygen in the atmosphere forming an oxide layer on the surface of the alloy, which hampers the growth of uniform nuggets in the weld. The oxide layer induces high contact resistance on the surface of the aluminum alloy, generating a large amount of heat, which may cause contamination of the electrode tip and deterioration of the welding quality.

Various studies have been carried out to obtain a reliable weld via uniform decomposition of the oxide layer on the aluminum alloy surface during the RSW process. Auhl and Patrick have reported that high electrode forces are required for aluminum alloys to remove the aluminum oxide layer during RSW [3]. In addition, many researchers have studied the effect of aluminum sheet surface conditions on the resistance spot weldability. For instance, Ronnhult et al. have studied the effect of the surface condition on the resistance spot weldability of the aluminum 5252 alloy [4] by comparing the weldability of the as-received specimens with that of the specimens pickled in NaOH and oxalic acid. They have reported that excellent weldability can be achieved by removing the oxide layer through pickling. Similarly, Li et al. have investigated the effects of sheet surface conditions on the electrode life during RSW on a 5A02 aluminum sheet [5]. A comparative study of the electrode lifetime performed using three surface treatment conditions, i.e., chemical cleaning, degreasing, and electric-arc cleaning, indicated that degreasing is the most practical method and may be suitable for automotive. Moreover, Han et al. have studied the effects of surface conditions on the resistance spot weldability of aluminum 5754 and 6111 alloys [6]. They recommend a 'full cleaning' process to prevent sticking and also report that the usable welding range can be extended using a closure sheet with electro-discharge texture (EDT).

Studies have been conducted to improve the resistance spot weldability of aluminum alloys by modifying the surface conditions of the electrode tip rather than the surface conditions of the aluminum alloy sheets. For instance, Sigler et al. have investigated the weldability of aluminum 6111 and 5754 alloys using electrodes with a multiring design on the surface [7]. This multiring electrode deforms the aluminum sheet surface upon contact and destroys the oxide layer on the aluminum surface, leading to a stable aluminum spot welding process. In addition, Kang et al. have investigated the resistance spot weldability and fatigue behavior of an aluminum 5754 wrought sheet and an Aural 2 die casting sheet using a multiring domed electrode [8]. They have found that the nugget size, which affects the tensile and bending strength, dominates the fatigue life. Moreover, Muller et al. have studied the effects of grinding, polishing, milling, and sandblasting on the electrode lifetime during RSW of aluminum 5182 alloy [9]. Jo et al. have investigated the effects of electrode face radius and force on the resistance spot weldability of aluminum 6061 alloy [10]. They have found that the optimal welding current range increases under a large electrode force. Previous studies were mainly focused on the effects of surface conditions on the resistance spot weldability of aluminum sheets. However, no systematic studies have been conducted on the influence of the electrode surface roughness and force on the resistance spot weldability of aluminum alloys.

The purpose of this study was to investigate the effects of electrode surface roughness and force on the resistance spot weldability and sticking of the electrode during RSW of aluminum 6061-T6 alloy. Accordingly, RSW was performed using two electrodes with different surface roughness under two different electrode forces, and the tensile shear strength, hardness, and nugget size of the welds were measured. In addition, the microstructures of the welds obtained with both electrodes were

analyzed. Electrode sticking was determined by performing a continuous RSW test up to 50 welds with the two electrodes and forces, separately.

2. Materials and Methods

The aluminum 6061-T6 alloy (sheet thickness = 1.5 mm) was used as the base material (BM). Table 1 lists the chemical composition and mechanical properties of the alloy. The alloy used in this study had a maximum tensile strength of 338 MPa and an elongation of 11%. The welding experiments were carried out using a medium-frequency direct-current (MFDC) RSW machine. Figure 1 shows the configuration of the welding electrode used in this study. The size of the electrode used for welding the 1.5 mm-thick aluminum alloy sheet was fixed according to the American Welding Society (AWS) standard. The outer diameter and radius of the electrodes for RSW were 20 mm and 50 mm, respectively. The surface of the abraded electrode was processed by sanding in one direction using 40-grit sandpaper. The surface roughness (R_a) of the as-received electrode was about $0.23 \mu\text{m}$, and the surface roughness of the abraded electrode was $4.66 \mu\text{m}$. Table 2 lists the welding conditions applied in this study. The welding conditions presented in Table 2 were determined through the weld lobe for the same base material using the as-received electrode. To investigate the effect of the electrode force on the various properties of the weld and the continuous RSW process, two electrode forces of 400 kgf and 600 kgf were selected. The welding currents were set to 32 kA and 36 kA for electrode forces of 400 kgf and 600 kgf, respectively. The welding time was fixed to 83.5 ms in all experiments. To evaluate the effect of the electrode surface roughness on the weldability, a continuous RSW process was performed using the as-received electrode and an abraded electrode. Subsequently, the nugget size, tensile shear strength, and hardness of the welds were measured. Moreover, a carbon imprint test was performed to investigate the electrode sticking during the continuous RSW process. The microstructures of the welds were observed using an optical microscope (OM).

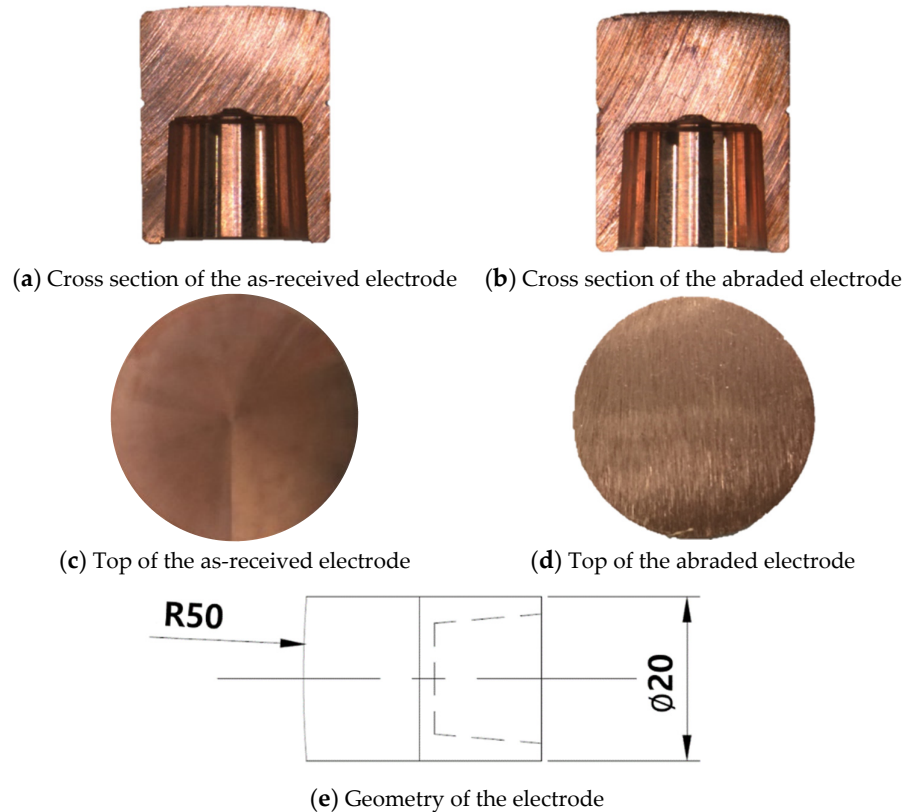


Figure 1. Configuration of the electrodes used in this study.

Table 1. Chemical composition and mechanical properties of aluminum alloy 6061-T6 used in this study.

Material	Chemical Composition (wt. %)								Mechanical Properties		
	Si	Fe	Cu	Mn	Mg	Cr	Ti	Al	yield strength (MPa)	tensile strength (MPa)	Elongation (%)
Al 6061-T6	0.59	0.39	0.25	0.07	1.12	0.19	0.03	Bal.	298	338	11

Table 2. Welding conditions used in this study.

Electrode Surface Type	Electrode Force (kgf)	Welding Current (kA)	Welding Time (ms)
as-received	400	32	83.5
abraded	600	36	

3. Results and Discussion

3.1. Nugget Size and Tensile Shear Strength

Table 3 lists the nugget size and tensile shear strength values of the resistance spot welds obtained using two different electrodes. When the as-received electrode was used, nuggets with sizes 7.2 mm and 8.2 mm were formed at the electrode forces of 400 kgf and 600 kgf, respectively; thus, the nugget size was slightly larger at the electrode force of 600 kgf. On the other hand, when the abraded electrode was used, nuggets with sizes 7.04 mm and 6.90 mm were formed at the electrode forces of 400 kgf and 600 kgf, respectively. Thus, comparatively larger nuggets were formed when the as-received electrode was used. The tensile shear strengths of the welds obtained with the as-received electrode were 4.99 kN and 4.89 kN at 400 kgf and 600 kgf, respectively. Even when including the error, the difference could be considered negligible. On the other hand, when the abraded electrode was used, welds with tensile shear strengths 4.37 kN and 4.23 kN were produced at 400 kgf and 600 kgf, respectively. Compared to the welds produced with the as-received electrode, those produced with the abraded electrode had lower tensile shear strengths. The weld nuggets formed with the as-received electrode were larger than those formed with the abraded electrode; therefore, the tensile shear strengths of the welds obtained using the as-received electrode were relatively larger.

Table 3. Tensile shear strength and nugget size of welds produced using electrodes with different surface roughness and at different electrode forces.

Electrode Surface Type	Electrode Force (kgf)	Welding Current (kA)	Welding Time (ms)	Tensile Shear Strength (kN)	Nugget Size (mm)
as-received	400	32	83.5	4.99 ± 0.08	7.20 ± 0.32
	600	36	83.5	4.89 ± 0.24	8.20 ± 0.04
abraded	400	32	83.5	4.37 ± 0.02	7.04 ± 0.01
	600	36	83.5	4.23 ± 0.02	6.90 ± 0.02

3.2. Hardness

The hardness measurements were carried out a day after welding to prevent age-hardening of the specimens. Figures 2 and 3 show the hardness test results of the welds obtained using the as-received and abraded electrodes at 400 kgf and 600 kgf. As shown in Figure 2, at the electrode force of 400 kgf, the average hardness values of the fusion zones (FZs) formed with the as-received and abraded electrodes were 55 HV and 59 HV, respectively. The hardness of the base material was about 95 HV. In addition, the hardness of the heat-affected zone (HAZ) produced with both the electrodes was about 80 HV. On the other hand, at the electrode force of 600 kgf, the hardness of the FZs produced using the as-received and abraded electrodes were 59 HV and 61 HV, respectively, excluding the defect in the nugget center, as shown in Figure 3. Moreover, the HAZ hardness values

were similar to those measured at the electrode force of 400 kgf. These results show that the weld hardness was not significantly affected by the electrode force or surface roughness.

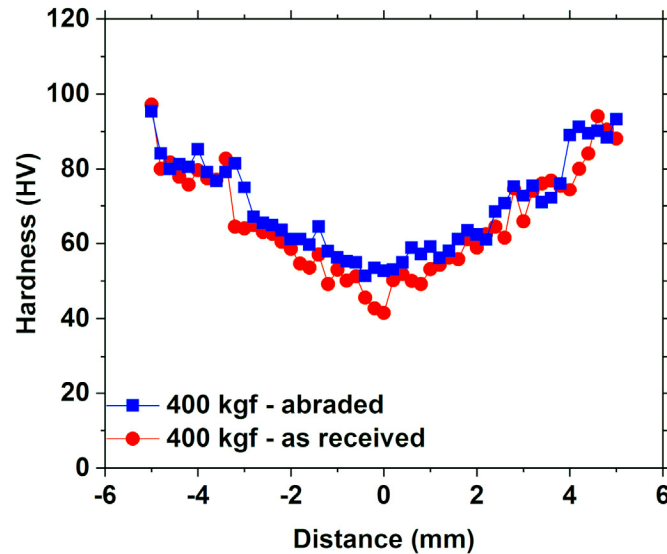


Figure 2. Measured hardness distribution of welds produced at the electrode force of 400 kgf.

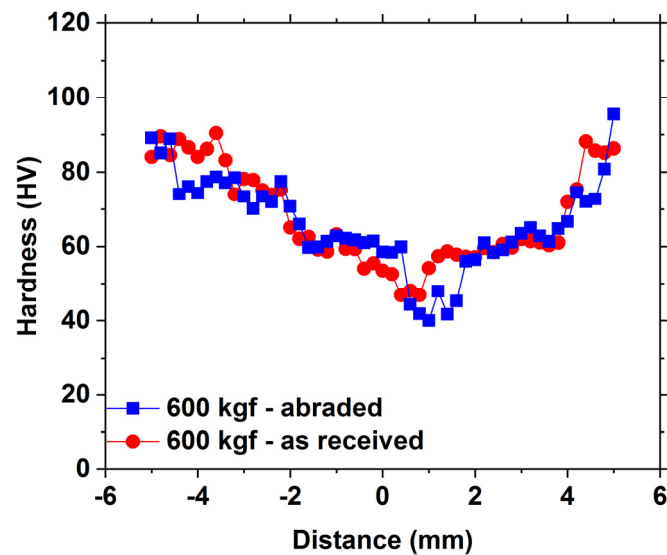


Figure 3. Measured hardness distribution of welds produced at the electrode force of 600 kgf.

3.3. Microstructure

The microstructure of the resistance spot weld could be divided into three zones, i.e., BM, HAZ, and FZ. Figure 4 shows the microstructure of the aluminum 6061-T6 matrix, as observed with the OM. The base material mainly consisted of grains elongated in the rolling direction, as shown in the figure. Figures 5 and 6 show the microstructures of the HAZ and FZ of the welds produced with the as-received and abraded electrodes, respectively. As shown in Figure 5a,b, the microstructure did not exhibit any partially melted zone at the electrode force of 400 kgf; however, a partially melted zone was observed near the columnar grain zone in the microstructure formed under 600 kgf. In addition, at the center of the FZ, an equiaxed grain zone was observed, as shown in Figure 5c,d; however, the grain size did not considerably change with the electrode force. The microstructures of the welds produced using the abraded electrode were not significantly different from those produced with the

as-received electrode. As shown in Figure 6a,b, a columnar grain zone and an HAZ were observed on either sides of the fusion line; in addition, a partially melted zone was observed. Moreover, in the center of the FZ, an equiaxed grain zone was observed (Figure 6c,d). As shown, the weld microstructure was not significantly affected by the electrode surface roughness. The grain size decreased from the HAZ, to the base material and finally the fusion zone.

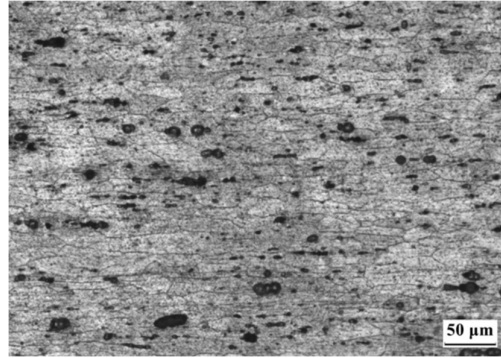


Figure 4. Microstructure of the base material used in this study.

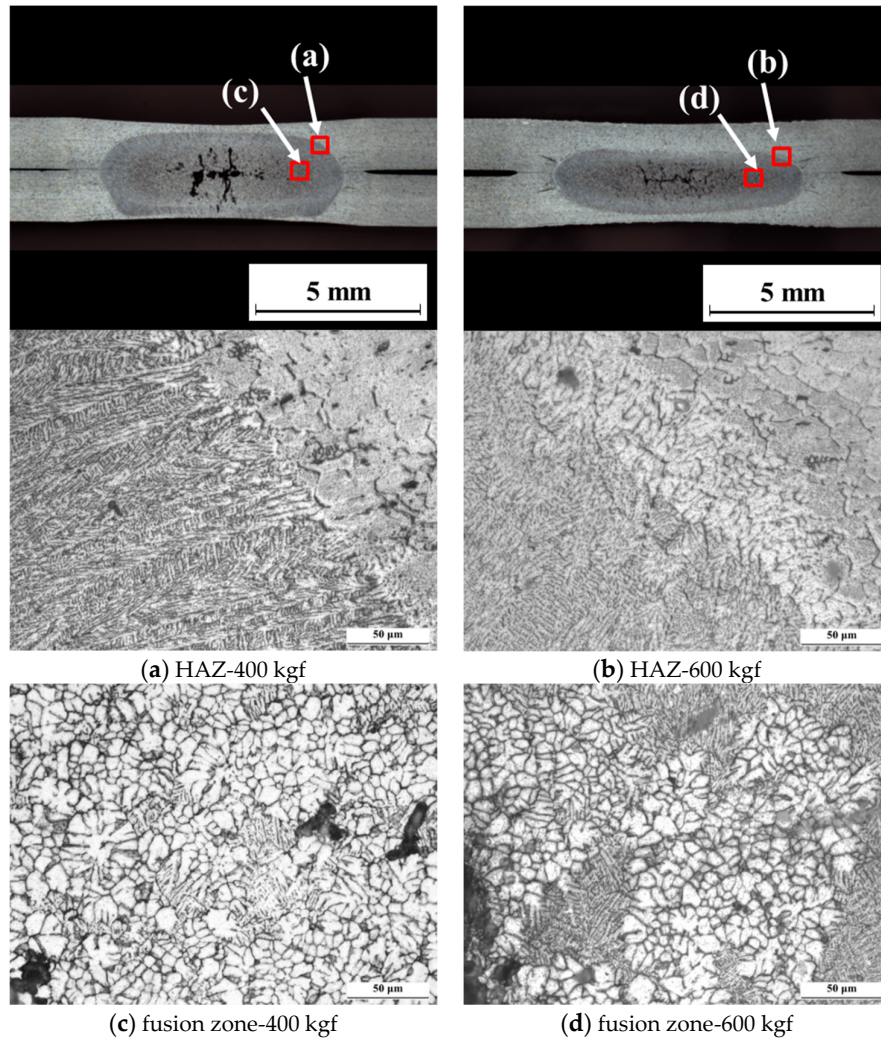


Figure 5. Microstructures of heat-affected zone (HAZ) and fusion zone obtained with the as-received electrode at electrode forces of 400 kgf and 600 kgf.

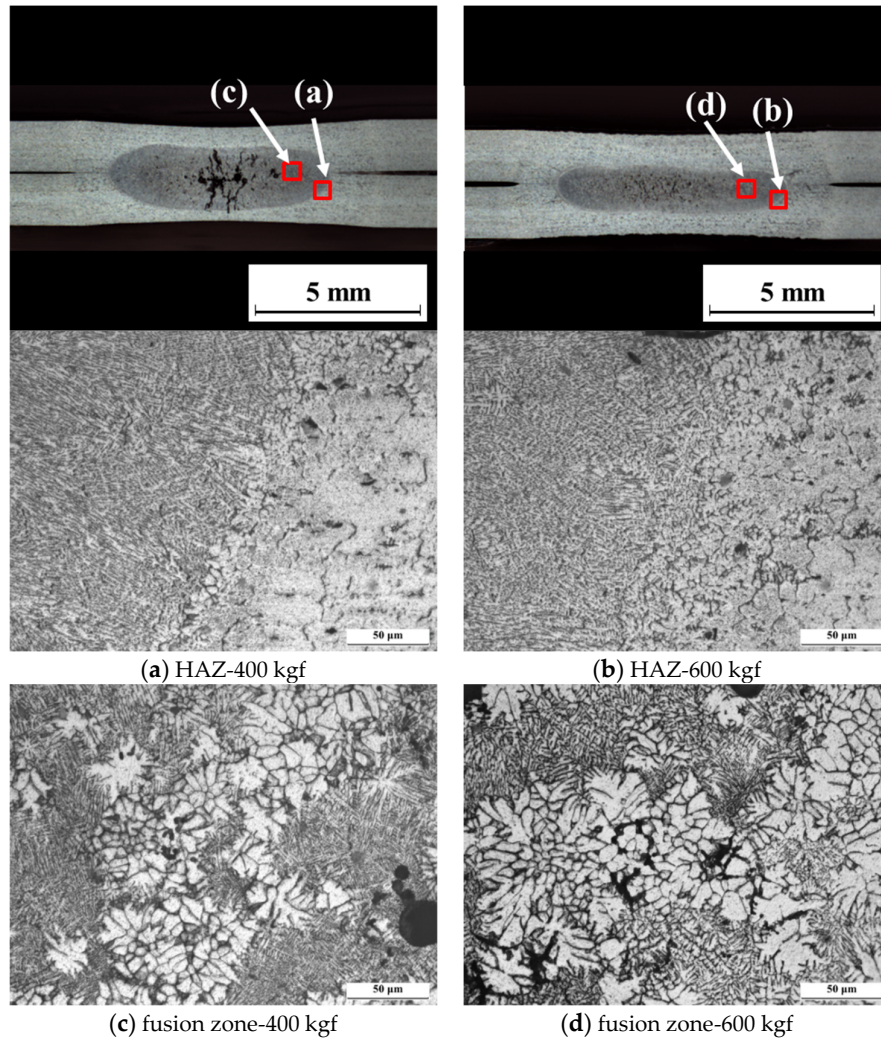


Figure 6. Microstructures of HAZ and fusion zone obtained with the abraded electrode at electrode forces of 400 kgf and 600 kgf.

3.4. Continuous Welding Process and Electrode Sticking

The nugget sizes and tensile shear strengths of the welds produced using the as-received and abraded electrodes were compared to investigate the influence of the electrode surface roughness on the weldability during the continuous RSW process, which was performed up to 50 welds. Nugget size and tensile shear strength were measured at intervals of five welds. Figure 7 shows the nugget size measurement results corresponding to the different electrodes, during the continuous RSW process at 400 kgf. All welds produced with the as-received electrode comprised nuggets with sizes between 7 mm and 7.5 mm. However, when the abraded electrode was used, at weld numbers 7, 22, and 27, nuggets of about 6 mm were formed, and at all other weld numbers, nuggets of about 7 mm were formed, similar to the nuggets produced with the as-received electrode. Figure 8 shows the size of the nuggets formed at 600 kgf. For the welds produced with the as-received electrode, the nuggets were larger than 7.5 mm, except at weld number 37. On the other hand, the nugget size of welds obtained using the abraded electrode was 7.0 mm or more, except at weld number 12. Overall, the nuggets produced with the as-received electrode were slightly larger than those produced with the abraded electrode.

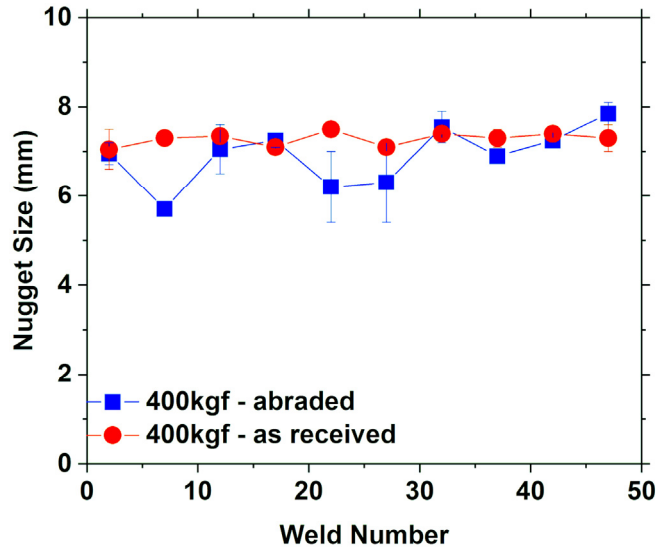


Figure 7. Measured nugget size during continuous resistance spot welding (RSW) under the electrode force of 400 kgf.

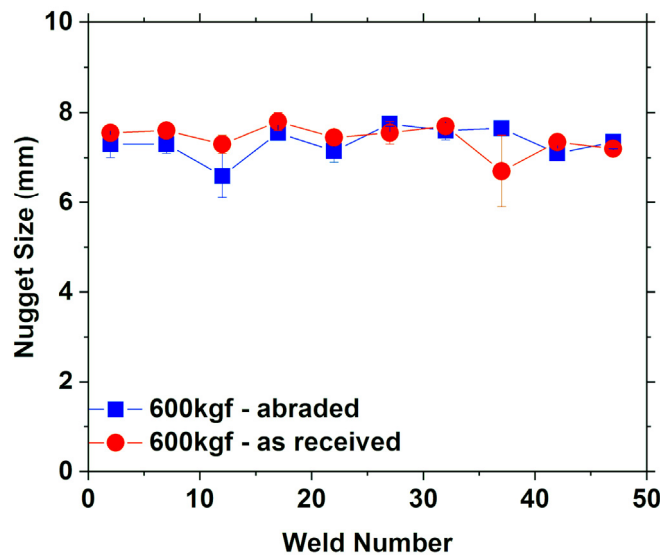


Figure 8. Measured nugget size during continuous RSW under the electrode force of 600 kgf.

Figures 9 and 10 show the effects of the electrode force and surface type on the tensile shear strength. At 400 kgf, the tensile shear strength of welds produced with the two electrodes was similar, i.e., between 4.5 kN and 5.0 kN, except at weld number 1 (Figure 9). However, at 600 kgf (Figure 10), the tensile shear strength of the welds produced with the as-received electrode was larger than 5.0 kN (up to weld number 40) and was slightly larger than that of the welds produced with the abraded electrode. As shown, there was no significant difference in the nugget size and tensile shear strength with variations in the electrode force and electrode surface type. Nevertheless, the tensile shear strength and nugget size of the welds produced with the as-received electrode were slightly larger than those of the welds produced with the abraded electrode. The Al_2O_3 oxide layer on the aluminum base material could be broken in the case of the abraded electrode because it had a rougher surface than the as-received electrode. Notably, it was more difficult to break the oxide film when using the as-received electrode than when using abraded electrode. Consequently, the contact resistance was

higher for the as-received electrode. This, in turn, led to an increase in the resistance heat and nugget size, which resulted in tensile shear strength enhancement.

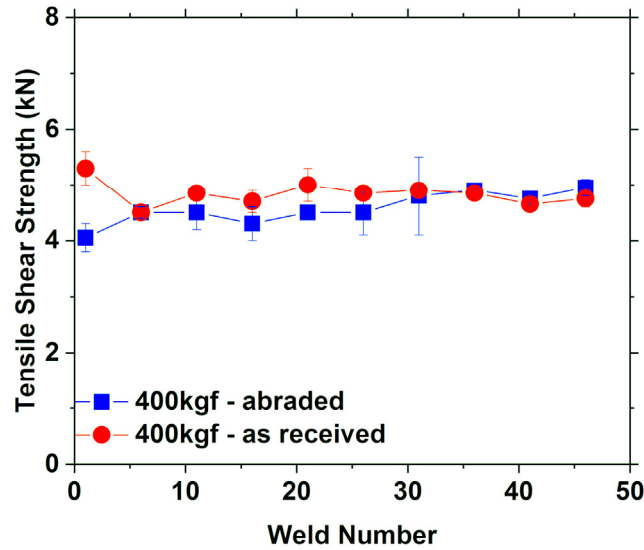


Figure 9. Measured tensile shear strength during continuous RSW under the electrode force of 400 kgf.

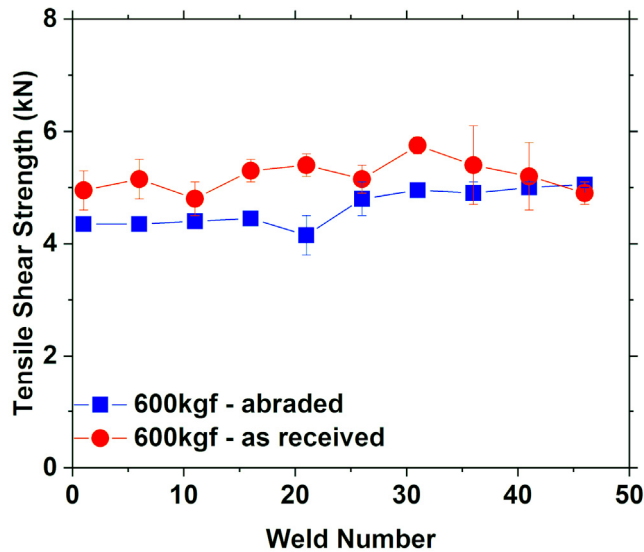


Figure 10. Measured tensile shear strength during continuous RSW under the electrode force of 600 kgf.

The effect of electrode surface roughness on electrode sticking was investigated using a carbon imprint test. Figures 11–14 show the results of the carbon imprint test performed on the (–) and (+) faces of the as-received and abraded electrodes at 400 kgf and 600 kgf. In the case of the as-received electrode, there was no significant change up to five welds at the electrode force of 400 kgf; however, sticking occurred on the (+) electrode face at weld number 10. Subsequently, sticking occurred on both the (–) and (+) electrode faces at weld number 15, and on all surfaces of the electrode at weld number 50. However, at 600 kgf, sticking first occurred at weld number 20, which was later than that at 400 kgf; moreover, sticking preferentially occurred at the (+) electrode face, similar to what observed at 400 kgf. On the other hand, in the case of the abraded electrode, sticking first occurred at

the (+) electrode face after about 35 welds at both 400 kgf and 600 kgf. In the case of the as-received electrode, the sticking of the electrode was alleviated by increasing the electrode force, as shown Figures 11 and 12. However, in the case of the abraded electrode, sticking at different electrode forces did not change significantly, as shown in Figures 13 and 14. Under the conditions of this study, this may be because the effect of the electrode surface roughness on the sticking of the electrode was greater than that of the electrode force. The difference in sticking between the (+) and (-) electrode faces was attributed to the thermoelectric effect, such as the Peltier effect, which causes a difference in the amount of heat generated, depending on the current direction when the current flows in the contact region between dissimilar metals [11]. More specifically, when a direct current (DC) flows through the two metals in contact with each other, a temperature difference occurs between the positive pole and the negative pole. This effect is referred to as the Peltier effect, results in wearing or sticking of the electrode, and can lead to the formation of irregularly shaped nuggets. Since the Peltier effect occurs when the current flows in only one direction, it can be solved by applying an alternating current (AC). Electrode sticking occurred because the nugget melted more rapidly in the thickness direction than in the radial direction of the base material during the continuous RSW process. Therefore, the effect of the electrode surface type on the growth of nuggets in the thickness direction of the base material was investigated.

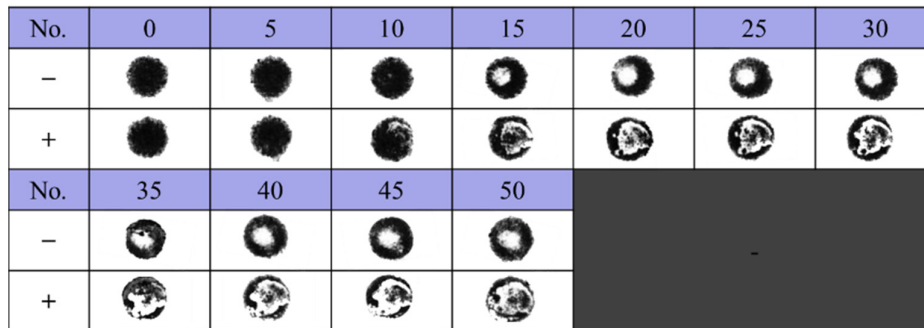


Figure 11. Carbon imprints of the as-received electrode at the electrode force of 400 kgf during continuous RSW.

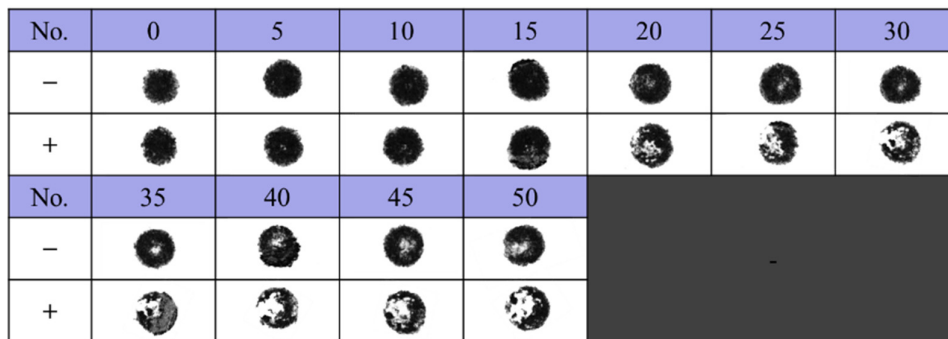


Figure 12. Carbon imprints of the as-received electrode at the electrode force of 600 kgf during continuous RSW.

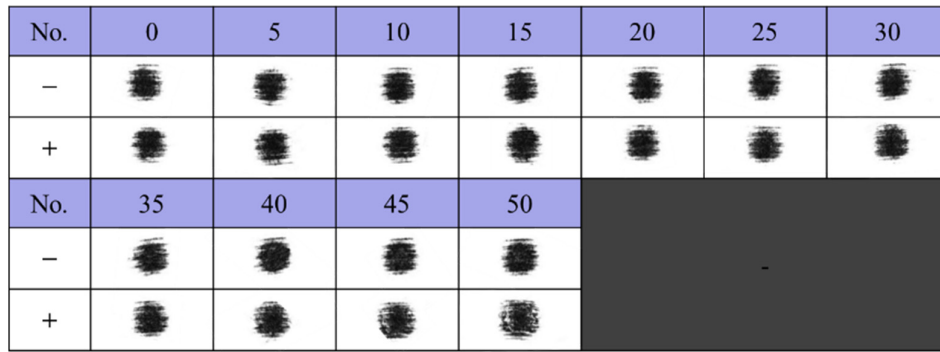


Figure 13. Carbon imprints of the abraded electrode at the electrode force of 400 kgf during continuous RSW.

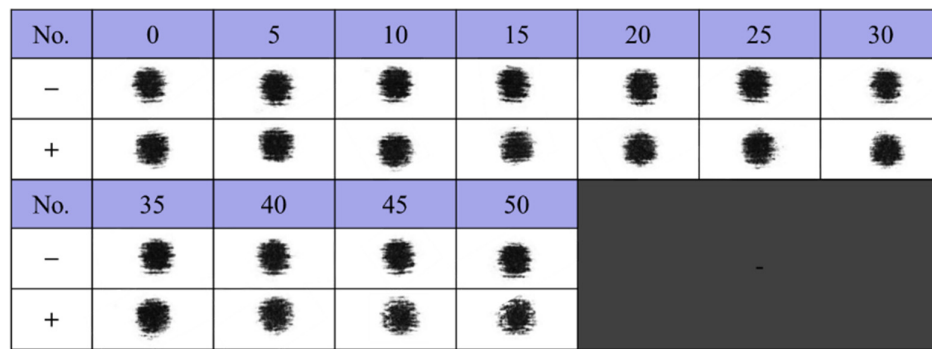
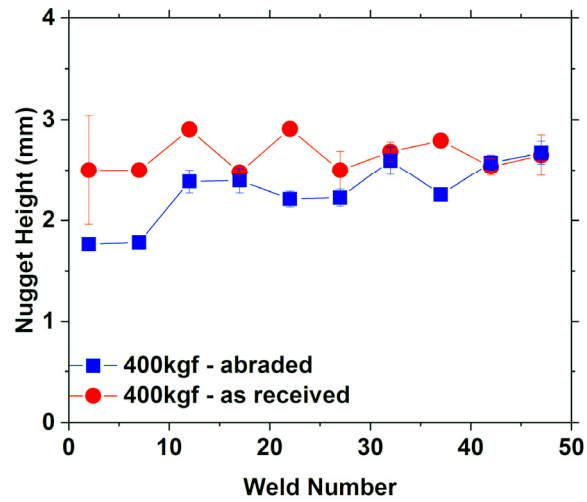


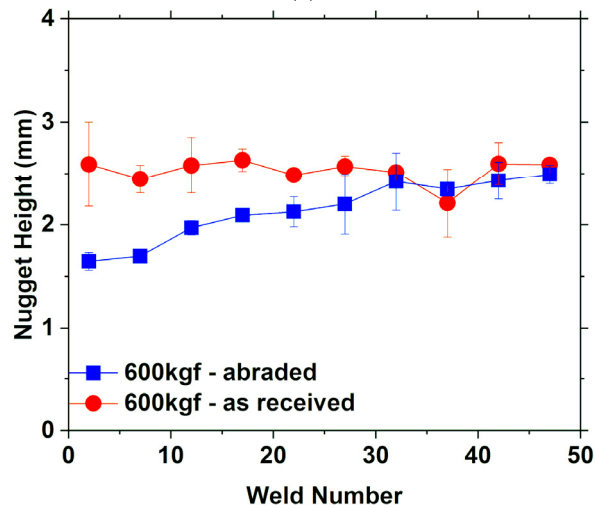
Figure 14. Carbon imprints of the abraded electrode at the electrode force of 600 kgf during continuous RSW.

Figures 15 and 16 show the nugget height and cross-section measurement results of welds produced with both the as-received and the abraded electrodes at different electrode forces during the continuous RSW process. At 400 kgf, the height of the nuggets produced with the as-received electrode was mostly 2.5 mm and it slightly increased at certain weld numbers. On the other hand, for the welds produced with the abraded electrode, the nugget height was about 1.7 mm at weld number 2, at 400 kgf and it gradually increased with increasing weld numbers; the height was about 2.6 mm at weld number 47. When the electrode force was increased to 600 kgf, the height of the nuggets produced with the as-received electrode was around 2.5 mm, except at weld number 37. For the welds produced with the abraded electrode, the nugget height was about 1.7 mm at weld number 2, similar to that measured under the electrode force of 400 kgf; however, the nugget height increased with the increase of the weld number, and its value was similar to that obtained using the as-received electrode at weld number 32. In the case of the as-received electrode, sticking occurred due to the nugget growth in the thickness direction and the melting of the base material over the entire thickness, as the weld number increased. In contrast, as shown in Figure 16, when the abraded electrode was used, the growth of the nugget in the thickness direction was slower compared to that observed for welds produced with the as-received electrode; therefore, the probability of sticking was reduced compared to the as-received electrode, because a molten layer did not develop on the surface of the base material. It was easy to remove the aluminum oxide film on the aluminum surface when using the abraded electrode during the RSW process because the surface roughness of the abraded electrode was higher than that of the as-received electrode. Figure 17 shows the measured dynamic resistance between the base material and the electrode according to the electrode type. As shown in Figure 17, the average dynamic resistances of the as-received electrode and the abraded electrode were 14.5 $\mu\Omega$ and 11.5 $\mu\Omega$ at welding time of 83.5 ms, respectively. The dynamic resistance was lower by 3 $\mu\Omega$ when the abraded electrode was used. The resistance between the abraded electrode and the

aluminum base material was small, and the resistance heat generated was low. In contrast, because the amount of heat generated between the as-received electrode and the base material due to the presence of the oxide layer was higher, the melting was enhanced during the welding process, which resulted in sticking of the electrode.

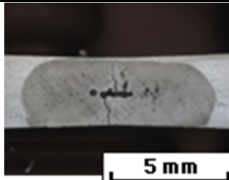
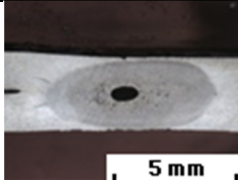


(a)



(b)

Figure 15. Measured height of the nuggets obtained using the as-received and the abraded electrodes at electrode forces of (a) 400 kgf and (b) 600 kgf.

Electrode type	Weld number 2	Weld number 47
As-received electrode		

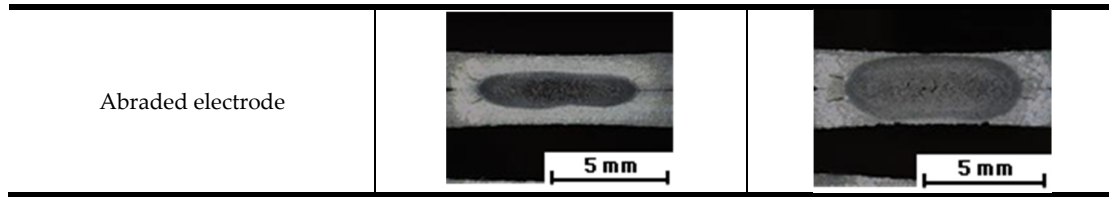


Figure 16. Cross sections of nuggets obtained using the as-received and the abraded electrodes during continuous RSW at electrode force of 600 kgf.

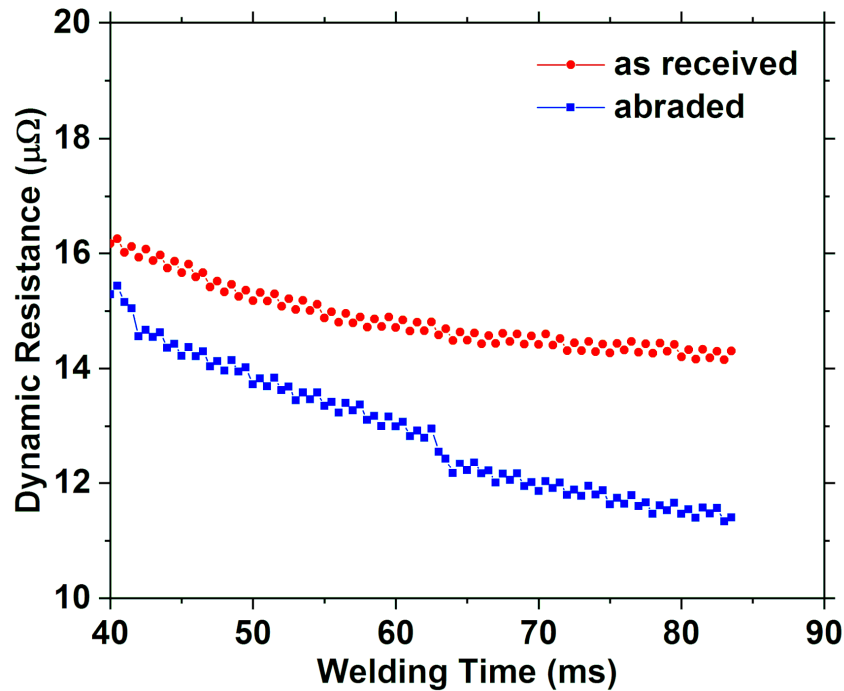


Figure 17. Measured dynamic resistance between base material and electrodes.

4. Conclusions

The effects of surface roughness and electrode force on the resistance point weldability of the aluminum 6061 alloy were investigated, and the following conclusions were drawn.

- (1) The electrode surface roughness (observed for the abraded electrode) allowed to destroy the oxide layer on the surface of the base material. As a result, the resistance heat between the base material and the electrode was reduced during resistance spot welding, so that the nugget size of the weld was reduced, and the tensile shear strength was reduced.
- (2) In the case of the as-received electrode, the sticking was slightly improved at a high electrode force, although it was very severe compared to that of the abraded electrode. In the case of the abraded electrode, the sticking was not affected by the electrode force. Therefore, the effect on the sticking of the electrodes according to the electrode force was more pronounced in the as-received electrode.
- (3) During the continuous RSW process using the abraded electrode with surface roughness, sticking of the electrode tip was delayed as compared to the as-received electrode. The sticking mainly occurred on the (+) electrode face because of thermoelectric effects such as the Peltier effect.
- (4) The increase of electrode surface roughness during the continuous RSW process reduced the sticking of the electrode by slowing the growth of the nugget in the thickness direction.

Author Contributions: Conceptualization, D.K. and Y.-M.K.; Investigation, H.J.; Methodology, D.K. and M.K.; Project administration, D.K.; Supervision, D.K., J.P. and Y.-M.K.; Writing—original draft, H.J.; Writing—review & editing, Y.-M.K.

Funding: This research was supported by funding from the Korea Institute of Industrial Technology.

Conflicts of Interest: The authors declare no conflict of interest.

References

1. Carle, D.; Blount, G. The Suitability of Aluminium as an Alternative Material for Car Bodies. *Mater. Des.* **1999**, *20*, 267–272.
2. Kim, G.-C.; Hwang, I.; Kang, M.; Kim, D.; Park, H.; Kim, Y.-M. Effect of welding time on resistance spot weldability of aluminum 5052 alloy. *Met. Mater. Int.* **2019**, *25*, 207–218.
3. Auhl, J.R.; Patrick, E.P. A fresh look at resistance spot welding of aluminum automotive components. *SAE Trans.: J. Mater. Manuf.* **1994**, *103*, 36–48.
4. Ronnhult, T.; Rilby, U.; Olefjord, I. The surface state and weldability of aluminium alloys. *Mater. Sci. Eng.* **1980**, *42*, 329–336.
5. Li, Z.; Hao, C.; Zhang, J.; Zhang, H. Effects of sheet surface conditions on electrode life in resistance welding aluminum. *Weld. J.* **2007**, *86*, 81–89.
6. Han, L.; Thornton, M.; Shergold, M. A comparison of the mechanical behavior of self-piercing riveted and resistance spot welded aluminum sheets for the automotive industry. *Mater. Des.* **2010**, *31*, 1457–1467.
7. Sigler, D.R.; Carlson, B.E.; Janiak, P. Improving aluminum resistance spot welding in automotive structures. *Weld. J.* **2013**, *92*, 64–72.
8. Kang, J.; Chen, Y.; Sigler, D.; Carlson, B.E.; Wilkinson, D.S. Fatigue behavior of dissimilar aluminum alloy spot Welds. *Procedia Eng.* **2015**, *114*, 149–156.
9. Mueller, M.; Cramer, H.; Bschorr, T. Optimization of the electrode processing methodology for resistance spot welding of aluminium. *Adv. Mater. Res.* **2013**, *814*, 147–158.
10. Jo, H.; Kim, Y.M.; Kang, M.; Kim, D. Effects of electrode face radius and force on resistance spot weldability of aluminum alloy 6061. *J. Weld. Join.* **2018**, *12*, 46–51.
11. Balder, T.C. Influence of the peltier effect in resistance welding. *Philips Tech. Rev.* **1958**, *20*, 188–192.



© 2019 by the authors. Licensee MDPI, Basel, Switzerland. This article is an open access article distributed under the terms and conditions of the Creative Commons Attribution (CC BY) license (<http://creativecommons.org/licenses/by/4.0/>).